Research Article | Vol. 32, No. 10 / 6 May 2024 / Optics Express 16790
Optics EXPRESS

Polarimetric measurement of temporal coherence in electromagnetic light beams

JYRKI LAATIKAINEN,[1,*] KIMMO SAASTAMOINEN,[1] ANDREAS NORRMAN,[1] JOSÉ J. GIL,[2] ARI T. FRIBERG,[1] AND TERO SETÄLÄ[1]

[1] *Center for Photonics Sciences, University of Eastern Finland, P.O. Box 111, FI-80101 Joensuu, Finland*
[2] *Department of Applied Physics, University of Zaragoza, Pedro Cerbuna 12, 50009 Zaragoza, Spain*
[*] *jyrki.laatikainen@uef.fi*

Abstract: We present a method to determine the degree of temporal coherence of a quasi-monochromatic vectorial light beam by polarimetric measurements. More specifically, we employ Michelson's interferometer in which the polarization Stokes parameters of the output (interference) beam are measured as a function of the time delay. Such a measurement enables us to deduce the magnitudes of the coherence (two-time) Stokes parameters, and hence the degree of coherence, of the input beam. Compared to existing methods the current technique has the benefits that neither optical elements in the arms of the interferometer nor visibility measurements are needed. The method is demonstrated with a laser diode and a filtered halogen source of various degrees of polarization.

1. Introduction

Coherence is a fundamental characteristic of light fields [1] and its importance is evident in areas such as interferometry, astronomy, correlation imaging, and medical optics [2]. In particular, the characterization of optical coherence in vectorial light fields [3] has been in the spotlight of modern photonics research due to its central role, e.g., in nanoscale optical interactions [4]. The current work contributes to this progress and presents a polarimetric method based on Michelson's interferometer [5] to measure the temporal coherence [6–8] of a random electromagnetic beam with a variable degree of polarization. In contrast to previous analogous experiments with vector light [9,10], the arms of the interferometer are empty which reduces error sources that could influence the interference field. Further, the method has an important difference and advantage compared to traditional coherence measurements [1,8,11–17] that no visibilities need to be extracted. The method is valid for quasimonochromatic fields with an arbitrary state of coherence and polarization, and it is demonstrated by experiments with a filtered halogen-lamp and a laser-diode source of different degrees of polarization.

2. Temporal coherence of electromagnetic beams

Consider a random, stationary (and ergodic), quasimonochromatic beam that propagates along the z axis and which is generally (uniformly) partially polarized. A realization of the electric field at time t is $\mathbf{E}(t) = \left[E_x(t), E_y(t)\right]^{\mathrm{T}}$, where $E_x(t)$ and $E_y(t)$ are the transverse components and T denotes transpose. The temporal coherence characteristics of the field at a time difference τ are described by the 2×2 mutual electric coherence matrix $\boldsymbol{\Gamma}(\tau) = \langle \mathbf{E}^*(t)\mathbf{E}^{\mathrm{T}}(t+\tau)\rangle$ [1,18], where the angle brackets and asterisk stand for time (or ensemble) averaging and complex conjugation, respectively. An equivalent representation of temporal coherence is provided by the coherence (two-time) Stokes parameters [19,20]

$$\mathcal{S}_n(\tau) = \mathrm{tr}\,[\boldsymbol{\sigma}_n \boldsymbol{\Gamma}(\tau)], \quad n = 0, \ldots, 3, \tag{1}$$

#507950 https://doi.org/10.1364/OE.507950
Journal © 2024 Received 10 Oct 2023; revised 4 Mar 2024; accepted 7 Mar 2024; published 23 Apr 2024

Optics EXPRESS

where tr denotes matrix trace, $\boldsymbol{\sigma}_0$ is the 2×2 identity matrix, and $\boldsymbol{\sigma}_1$, $\boldsymbol{\sigma}_2$, $\boldsymbol{\sigma}_3$ are the Pauli spin matrices [1]. At $\tau = 0$, these parameters reduce to the polarization Stokes parameters $S_n = \mathrm{tr}\,(\boldsymbol{\sigma}_n \mathbf{J})$, where $\mathbf{J} = \boldsymbol{\Gamma}(0)$ is the time-domain polarization matrix [1]. Employing the intensity-normalized coherence Stokes parameters $\gamma_n(\tau) = \mathcal{S}_n(\tau)/S_0$, the electromagnetic degree of coherence, $\gamma(\tau)$, reads [6,7]

$$\gamma^2(\tau) = \frac{\mathrm{tr}\,[\boldsymbol{\Gamma}(\tau)\boldsymbol{\Gamma}(-\tau)]}{\mathrm{tr}^2\mathbf{J}} = \frac{1}{2}\sum_{n=0}^{3} |\gamma_n(\tau)|^2. \tag{2}$$

This quantity is real and bounded as $0 \leq \gamma(\tau) \leq 1$ with the lower and upper limit corresponding to temporal incoherence and complete temporal coherence, respectively.

The beam enters into a Michelson interferometer (Fig. 1) where it is divided into two portions by a 50:50 beam splitter. The two fields travel the distances L_1 and L_2 to the mirrors in arms 1 and 2. After reflections the beams propagate back to the beam splitter and are recombined. The output field is given as

$$\mathbf{E}'(t) = \mathbf{E}_1(t) + \mathbf{E}_2(t), \tag{3}$$

where $\mathbf{E}_1(t)$ and $\mathbf{E}_2(t)$ are the beams from the arms 1 and 2. These are connected to the incident field as [9]

$$\mathbf{E}_1(t) = \frac{1}{\sqrt{2}}\mathrm{e}^{\mathrm{i}\phi_2}\mathbf{C}\frac{1}{\sqrt{2}}\mathbf{C}\mathrm{e}^{\mathrm{i}\phi_1}\mathbf{E}(t - t_0) = \frac{1}{2}\mathrm{e}^{\mathrm{i}(\phi_1+\phi_2)}\mathbf{E}(t - t_0), \tag{4}$$

$$\mathbf{E}_2(t) = \frac{1}{\sqrt{2}}\mathbf{C}\mathrm{e}^{\mathrm{i}\phi_4}\mathbf{C}\frac{1}{\sqrt{2}}\mathrm{e}^{\mathrm{i}\phi_3}\mathbf{E}(t - t_0 - \tau) = \frac{1}{2}\mathrm{e}^{\mathrm{i}(\phi_3+\phi_4)}\mathbf{E}(t - t_0 - \tau), \tag{5}$$

where $\mathbf{C} = \mathrm{diag}\,[-1, 1]$ accounts for the reflections on the beam splitter and mirrors [9,21], $\phi_1, \ldots, \phi_4$ denote the (deterministic) phase shifts induced by the reflections and transmissions at the beam splitter, and t_0 is the propagation time in the interferometer when the arms are of equal length. Note that $\mathbf{E}_2(t)$ depends on the time delay $\tau = 2(L_2 - L_1)/c$ due to the path length difference, with c being the speed of light. The polarization matrix $\mathbf{J}'(\tau) = \langle \mathbf{E}'^*(t)\mathbf{E}'^{\mathrm{T}}(t)\rangle$ of the output beam is

$$\mathbf{J}'(\tau) = \mathbf{J}_1 + \mathbf{J}_2 + \langle \mathbf{E}_1^*(t)\mathbf{E}_2^{\mathrm{T}}(t)\rangle + \langle \mathbf{E}_2^*(t)\mathbf{E}_1^{\mathrm{T}}(t)\rangle, \tag{6}$$

where $\mathbf{J}_1 = \langle \mathbf{E}_1^*(t)\mathbf{E}_1^{\mathrm{T}}(t)\rangle$ and $\mathbf{J}_2 = \langle \mathbf{E}_2^*(t)\mathbf{E}_2^{\mathrm{T}}(t)\rangle$, which via Eqs. (4) and (5) are found to satisfy $\mathbf{J}_1 = \mathbf{J}_2 = \mathbf{J}/4$. The first term expressing the mutual correlation of $\mathbf{E}_1(t)$ and $\mathbf{E}_2(t)$ in Eq. (6) has the form $\langle \mathbf{E}_1^*(t)\mathbf{E}_2^{\mathrm{T}}(t)\rangle = \mathrm{e}^{\mathrm{i}\Delta\phi}\boldsymbol{\Gamma}(-\tau)/4$, where $\Delta\phi = \phi_3 + \phi_4 - \phi_1 - \phi_2$. Hence, Eq. (6) can be reformulated as

$$\mathbf{J}'(\tau) - \frac{1}{2}\mathbf{J} = \frac{1}{4}[\mathrm{e}^{-\mathrm{i}\Delta\phi}\boldsymbol{\Gamma}(\tau) + \mathrm{e}^{\mathrm{i}\Delta\phi}\boldsymbol{\Gamma}^\dagger(\tau)], \tag{7}$$

where the dagger denotes the Hermitian adjoint. Note that above the polarization matrix $\mathbf{J}'(\tau)$ of the output beam is a function of the time difference τ, whereas the matrix $\mathbf{J}$ pertaining to the input beam is independent of τ. In terms of the polarization and coherence Stokes parameters this yields

$$2S_n'(\tau) - S_n = \mathrm{Re}[\mathrm{e}^{-\mathrm{i}\Delta\phi}\mathcal{S}_n(\tau)] = |\mathcal{S}_n(\tau)|\cos[\alpha_n(\tau) - \omega_0\tau - \Delta\phi], \tag{8}$$

where Re denotes the real part and ω_0 is an angular frequency within the spectral band of the beam (often the center frequency). In addition, $\alpha_n(\tau) = \arg[\mathcal{S}_n(\tau)] + \omega_0\tau$, where arg is the phase of a complex number. Since for quasimonochromatic beams $|\mathcal{S}_n(\tau)|$ and $\alpha_n(\tau)$ vary slowly as a function of τ, the Stokes parameters are sinusoidally modulated with the period $2\pi/\omega_0$. Hence, the magnitudes of $\mathcal{S}_n(\tau)$ can be determined by measuring $S_n'(\tau)$ and S_n polarimetrically and extracting the envelopes of $2S_n'(\tau) - S_n$ on the left side of Eq. (8). The electromagnetic degree of coherence can then be obtained using the latter equality in Eq. (2). The phases of the complex $\mathcal{S}_n(\tau)$ parameters could be obtained from the locations of the oscillating patterns inside the envelopes, although this is not considered in this work.

Research Article | Vol. 32, No. 10 / 6 May 2024 / Optics Express 16792
Optics EXPRESS

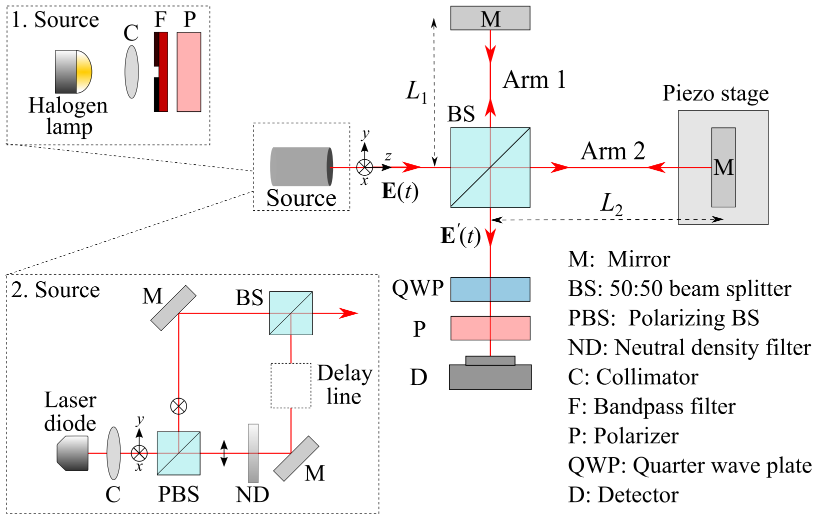

Fig. 1. Illustration of the source light preparation and Michelson's interferometer. Inset 1 shows a halogen lamp whose emission is collimated and spectrum filtered to a 10 nm bandwidth (FWHM). The output is unpolarized but can be made polarized with an additional polarizer. Inset 2 shows a laser-diode source whose output is collimated and divided into two orthogonal polarizations that propagate along different paths. The beam in one of the paths is delayed beyond the coherence length and its intensity is adjusted with a neutral density filter, after which the two beams are recombined. The prepared beam enters a Michelson interferometer where the path difference between the arms 1 and 2 is controlled with a piezo stage. The polarization Stokes parameters at the output are measured with a quarter-wave plate, polarizer, and CMOS camera.

3. Experimental setup

We demonstrate the above theory by measuring the degree of temporal coherence for two light sources, a halogen lamp and a laser diode (HL6388MG), whose spectra are presented in Fig. 2. The lamp spectrum was made narrower using a bandpass filter [center wavelength 632.8 nm, full width at half maximum (FWHM) 8.5 nm] as shown in the upper inset of Fig. 1. In addition, the diode source is operated just below the lasing threshold to ensure a sufficiently wide spectrum

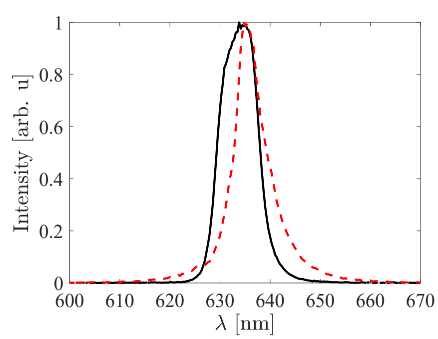

Fig. 2. Spectra of the considered light sources. Solid black curve: filtered light from a halogen lamp (center wavelength at 632.8 nm, FWHM 8.5 nm); dashed red curve: emission from a laser diode below the threshold (center wavelength at 634.8 nm, FWHM 6.5 nm).

Optics EXPRESS

(center wavelength 634.8 nm, FWHM 6.5 nm) which keeps the longitudinal coherence length within the micrometer scale. In the case of the halogen lamp, we consider the output with and without a polarizer (transmission axis in the x direction) corresponding to essentially unpolarized and fully polarized light, respectively. For the diode source, we apply a delay line to control the degree of polarization as illustrated in the lower inset of Fig. 1. Collimated light from the diode source is divided with a polarizing beam splitter into orthogonal linear polarization states which are guided into separate arms. The optical path in the lower arm is increased to exceed the longitudinal coherence length, ensuring no correlation between the outputs of the arms which are combined into a single beam with mirrors and a 50:50 non-polarizing beam splitter. Adjusting the beam intensity I_a in the lower arm with a neutral density filter enables us to control the degree of polarization according to $P = |I_a - I_b|/(I_a + I_b)$, where I_b is the intensity in the upper arm. In the experiments, three values for the diode light are considered: $P = 0$, $P = 0.68$, and $P = 1$, signifying unpolarized, partially polarized, and fully polarized light, respectively.

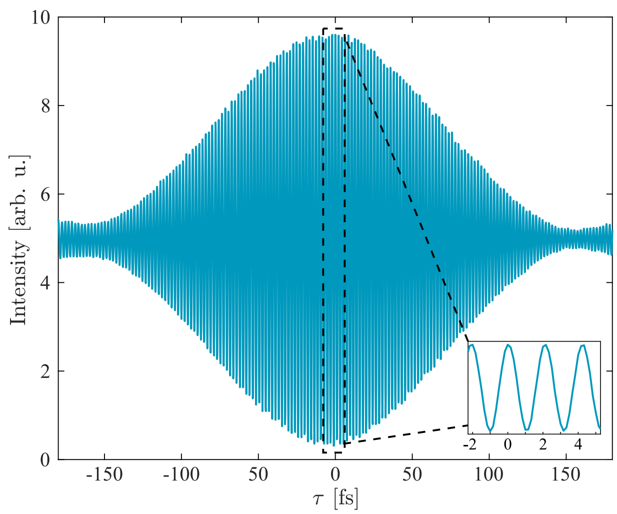

Fig. 3. Intensity $I_1(\tau)$ as a function of the time delay τ measured with a Michelson interferometer. The inset shows the behavior around $\tau = 0$.

The prepared source light is directed to a Michelson interferometer, depicted in Fig. 1, where the time delay in one of the arms is altered using a linear piezo stage (PI P-611.1) with an average step of 25 nm. The total scan length of the stage is adjusted to exceed the coherence length of the incident light. The recombined beam travels through a quarter-wave plate and a linear polarizer to a CMOS camera which captures the beam intensity at each piezo step. Measuring the intensity for four different mutual orientations of the wave plate and polarizer allows us to deduce the polarization Stokes parameters of the interference field as a function of τ. Specifically, the angle $\theta_{\rm wp}$ that the wave plate's fast axis and the angle $\theta_{\rm p}$ that the polarizer's transmission axis make with the x axis are chosen to be: $(\theta_{\rm wp}, \theta_{\rm p}) = (0°, 0°)$, $(0°, 45°)$, $(45°, 45°)$, and $(90°, 90°)$. Labelling the related intensities as $I_1(\tau), \ldots, I_4(\tau)$ the polarization Stokes parameters at the output of the interferometer can be written as [22]

$$S'_0(\tau) = I_1(\tau) + I_4(\tau), \tag{9}$$

$$S'_1(\tau) = I_1(\tau) - I_4(\tau), \tag{10}$$

$$S'_2(\tau) = 2I_3(\tau) - I_1(\tau) - I_4(\tau), \tag{11}$$

$$S'_3(\tau) = 2I_2(\tau) - I_1(\tau) - I_4(\tau). \tag{12}$$

Optics EXPRESS

These parameters are measured also when the light in one arm is blocked which provides $S_n/4$ for all $n = 0, \ldots, 3$. Constructing $2S'_n(\tau) - S_n$, extracting the envelopes, and utilizing Eq. (8) result in the magnitudes of the coherence Stokes parameters, $|\mathcal{S}_n(\tau)|$, of the input field.

As an example, a measured $I_1(\tau)$ is presented in Fig. 3 for the filtered, polarized light from the halogen lamp. The intensity is measured by summing over a few pixels in the beam cross section for each τ value. The distribution has the maximum close to $\tau = 0$ and exhibits rapid oscillations with the period of 2.1 fs corresponding to 630 nm (see the inset). Similar behavior is found for $I_2(\tau)$, $I_3(\tau)$, and $I_4(\tau)$ as well. In overall, the procedure described above was carried out at 50 locations in the vicinity of the beam center. Further, the coherence Stokes parameters and degree of coherence were calculated at each location and averaged over them. This process enables us to find and discard anomalies due to imperfections in the polarimetric components.

4. Measured temporal coherence of specific light sources

The magnitudes of the normalized coherence Stokes parameters for the halogen lamp without a polarizer are presented in Fig. 4(a). We see that only $|\gamma_0(\tau)|$ assumes significant nonzero values. This is expected since the light from the halogen lamp is virtually unpolarized and its temporal coherence is to a good approximation symmetric, in the sense that $\Gamma_{xx}(\tau) = \Gamma_{yy}(\tau)$ and $\Gamma_{xy}(\tau) = \Gamma_{yx}(\tau) = 0$, where $\Gamma_{ij}(\tau)$ $(i, j = x, y)$ are the elements of $\mathbf{\Gamma}(\tau)$. Figure 4(b) shows the degree of coherence as a function of τ given in Eq. (2). The maximum value (including the standard deviation) is $\gamma(0) \approx 0.647 \pm 0.004$, which is close to the theoretical maximum $1/\sqrt{2} \approx 0.707$ for a fully unpolarized beam [6].

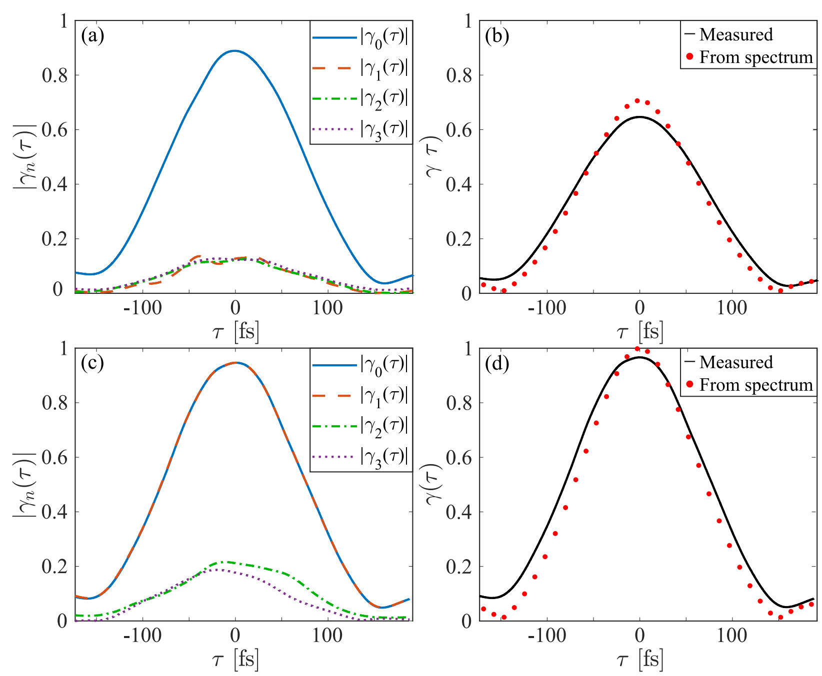

Fig. 4. Magnitudes of the normalized coherence Stokes parameters $\gamma_0(\tau), \ldots, \gamma_3(\tau)$ (left column) and the corresponding degrees of coherence $\gamma(\tau)$ (right column) as a function of the time difference τ for the filtered halogen source. Upper row: unpolarized light; lower row: polarized light. In the right column, solid curves are the measured quantities while dots are the values computed from the spectrum (solid black curve in Fig. 2).

Optics EXPRESS

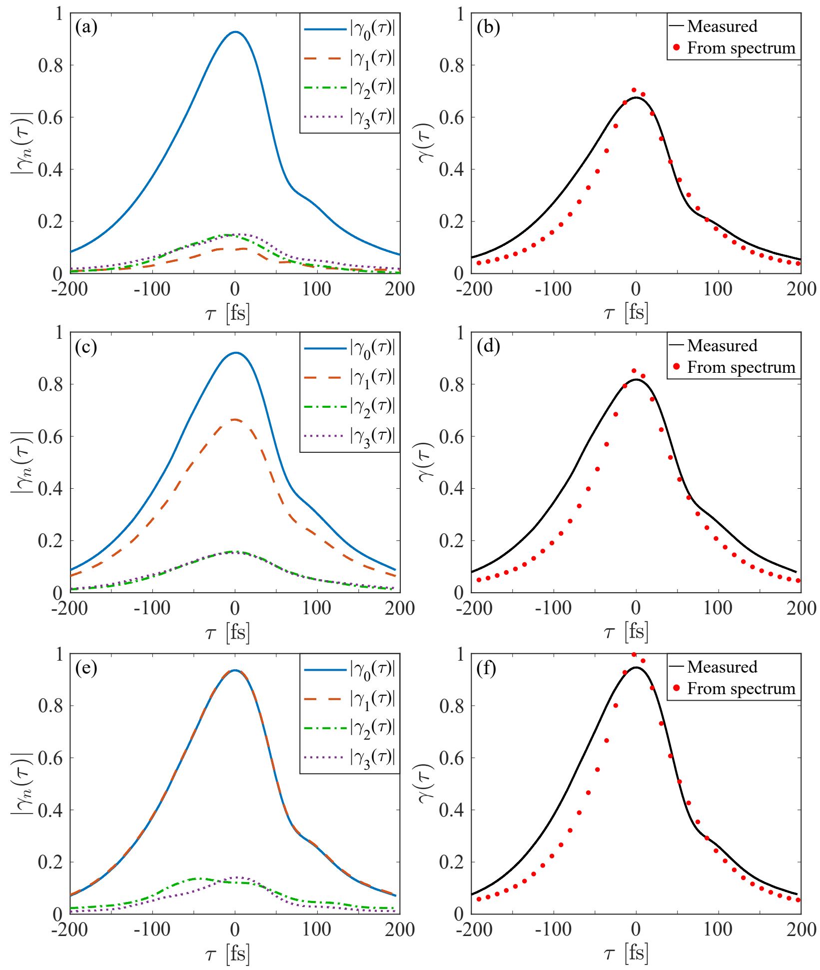

Fig. 5. Magnitudes of the normalized coherence Stokes parameters $\gamma_0(\tau), \ldots, \gamma_3(\tau)$ (left column) and the corresponding degrees of coherence $\gamma(\tau)$ (right column) as a function of the time difference τ for the laser diode operated just below the threshold. Upper row: unpolarized light ($P = 0$); middle row: partially polarized light ($P = 0.68$); lower row: polarized light ($P = 1$). Red dots on the right column correspond to the degree of coherence obtained from the spectrum (dashed red curve in Fig. 2) while the solid black lines indicate the measured values.

The half width of the half maximum (HWHM) of the peak, serving as an estimation of the coherence time of light, is about 82 fs. For comparison, the degree of coherence obtained from the source spectrum in Fig. 2 is shown with dots (calculations are found in the Appendix). Both methods are seen to be in agreement overall and consistent with the results on the filtered halogen light in [10] where the visibility measurements were employed. The difference in Fig. 4(b) originates from the fact that in the spectrum method (dots) the polarization properties are taken spectrally invariant, which is not exactly true in the experiment (solid curve) due to possible imperfections in the optical elements. Figure 4(c) shows the temporal coherence for the halogen lamp with a polarizer whose transmission axis is in the x direction. In this case, $|\gamma_0(\tau)| = |\gamma_1(\tau)|$, with notably larger values than $|\gamma_2(\tau)| \approx |\gamma_3(\tau)|$. The corresponding $\gamma(\tau)$ is depicted in Fig. 4(d), where $\gamma(0) \approx 0.966 \pm 0.013$ is close to the theoretical value of unity. The measured degree

Optics EXPRESS

of coherence is in agreement with that calculated from the spectrum (dots) and the HWHM is estimated to be 82 fs.

Figure 5 shows the polarimetric measurement of the normalized coherence Stokes parameters (left column) and degrees of coherence (right column) with a laser diode source for three different degrees of polarization: $P = 0$ (top row), $P = 0.68$ (middle row), and $P = 1$ (bottom row). In the cases of unpolarized and polarized light, Figs. 5(a) and (e), respectively, the behaviors of the coherence Stokes parameters are similar to those of the halogen lamp light in Fig. 4. The partially polarized light in Fig. 5(b) displays quite similar character as the fully polarized light in Fig. 5(e), with the difference that in the former case $|\gamma_1(\tau)|$ is smaller than in the latter case. The degrees of coherence $\gamma(\tau)$ as implied by the normalized coherence Stokes parameters are found to have the maximum values $\gamma(0) \approx 0.675 \pm 0.023$, $\gamma(0) \approx 0.818 \pm 0.037$, and $\gamma(0) \approx 0.947 \pm 0.035$ for the unpolarized, partially polarized, and fully polarized laser-diode beam, respectively. These are close to the corresponding theoretical values of $\gamma(0) \approx 0.707$, $\gamma(0) \approx 0.855$, and $\gamma(0) = 1$. Additionally, the related HWHM's are 68 fs, 73 fs, and 69 fs, which are similar to those of the halogen light. This is expected since the spectral widths are essentially the same in both cases. The slight deviations arise from the difference between the shapes of the spectra, which affects the HWHM's of the corresponding degrees of coherence due to the Fourier transform relationship shown in the Appendix. Finally, in the right column of Fig. 5, we compare the measured degrees of coherence of the diode sources with those obtained by Fourier transforming the spectrum. The agreement is good, with the differences arising from the imperfections in the optical elements, as in the case of the halogen source.

As a general observation we note that in all cases the measured maximum value $\gamma(0)$ is slightly smaller than the theoretical value. An obvious error source is that the wave plate may not work ideally throughout the spectra and possible nonuniformities in the plate may cause further effects. In addition, the beam splitters, polarizers, and filters likewise are not ideal. These contributions show up, e.g., in Fig. 3, where the intensity does not reach zero at $\tau = 0$. A similar effect was seen also in the approach of [10], where the visibilities of the Stokes-parameter modulations were evaluated to obtain the temporal coherence properties of various beams. We also emphasize that the current method has the benefit that the arms of the interferometer do not contain any optical elements which significantly reduces the number of possible error sources.

5. Conclusions

In conclusion, we presented an experimental method which enables one to measure the temporal degree of coherence of a quasimonochromatic vector-light beam by standard polarimetric means. Unlike in traditional coherence measurements no visibility detection is needed. This may be beneficial since such measurements are often highly sensitive especially close to the points of unit and zero visibilities. In particular, compared to previous coherence measurements with vector-light beams, no optical elements are employed in the arms of the interferometer, thus eliminating several error sources concerning the interference field. The procedure was demonstrated with a filtered halogen lamp and a laser-diode source with prepared degrees of polarization. The experimental results are in agreement with the theoretical ones as well as with the previous studies in the literature [10].

Appendix

This appendix describes the calculation of the degree of coherence from the spectrum. The spectrum (or spectral density) is defined as $S_0(\omega) = \mathrm{tr}\,[\mathbf{\Phi}(\omega)]$, where $\mathbf{\Phi}(\omega)$ is the spectral polarization matrix and tr denotes the trace. According to the Wiener–Khintchine theorem [1] the mutual coherence matrix is given by

$$\mathbf{\Gamma}(\tau) = \int_0^\infty \mathbf{\Phi}(\omega) e^{-i\omega\tau} d\omega, \tag{13}$$

where the lower limit conforms to the complex analytic signal representation. The above relation shows how spectral polarization affects electromagnetic temporal coherence. The characteristic decomposition of the spectral polarization matrix is written as [23]

$$\mathbf{\Phi}(\omega) = S_0(\omega)\left(\mathcal{P}\hat{\mathbf{a}}\hat{\mathbf{a}}^\dagger + \frac{1-\mathcal{P}}{2}\boldsymbol{\sigma}_0\right), \tag{14}$$

where $\mathcal{P}$ is the spectral degree of polarization and $\boldsymbol{\sigma}_0$ is the 2×2 unit matrix. In addition, $\hat{\mathbf{a}}$ is the eigenvector which corresponds to the larger eigenvalue of $\mathbf{\Phi}(\omega)$ and satisfies the properties $\mathrm{tr}(\hat{\mathbf{a}}\hat{\mathbf{a}}^\dagger) = 1$ and $\det(\hat{\mathbf{a}}\hat{\mathbf{a}}^\dagger) = 0$. In other words, Eq. (14) represents the spectral polarization matrix as a sum of matrices expressing polarized and unpolarized contributions at frequency ω [1]. In general, both $\mathcal{P}$ and $\hat{\mathbf{a}}$ depend on frequency but here we assume that they are constants over the narrow spectral bandwidths of the quasimonochromatic beams considered in the main text. Consequently, combining Eqs. (13) and (14) results in

$$\mathbf{\Gamma}(\tau) = \left(\mathcal{P}\hat{\mathbf{a}}\hat{\mathbf{a}}^\dagger + \frac{1-\mathcal{P}}{2}\boldsymbol{\sigma}_0\right) \int_0^\infty S_0(\omega) e^{-i\omega\tau} d\omega. \tag{15}$$

The time-domain polarization matrix is obtained at $\tau = 0$ as

$$\mathbf{J} = \left(\mathcal{P}\hat{\mathbf{a}}\hat{\mathbf{a}}^\dagger + \frac{1-\mathcal{P}}{2}\boldsymbol{\sigma}_0\right) \int_0^\infty S_0(\omega) d\omega. \tag{16}$$

It follows that the temporal degree of polarization, $P = \sqrt{1 - 4\det\mathbf{J}/\mathrm{tr}^2\mathbf{J}}$, equals the spectral counterpart, $P = \mathcal{P}$. This fact and substitution of Eqs. (15) and (16) into the first form in Eq. (2) lead to

$$\gamma(\tau) = \sqrt{\frac{1+P^2}{2}}\, \frac{\left|\int_0^\infty S_0(\omega) e^{-i\omega\tau} d\omega\right|}{\int_0^\infty S_0(\omega) d\omega}. \tag{17}$$

The above expression gives the degree of temporal coherence of a quasimonochromatic, partially polarized beam in terms of the spectrum and the degree of polarization under the condition of spectral polarization invariance. It was employed in the main text to compute the (red) dotted curves in Figs. 4 and 5.

Funding. Joensuu University Foundation; Research Council of Finland (349396, PREIN 320166, PROFI6 336119).

Disclosures. The authors declare no conflicts of interest.

Data Availability. Data underlying the results presented in this paper are not publicly available at this time but may be obtained from the authors upon reasonable request.

References

1. L. Mandel and E. Wolf, *Optical Coherence and Quantum Optics* (Cambridge University, 1995).
2. O. Korotkova and G. Gbur, "Applications of optical coherence theory," Prog. Opt. **65**, 43–104 (2020).
3. A. T. Friberg and T. Setälä, "Electromagnetic theory of optical coherence [Invited]," J. Opt. Soc. Am. A **33**(12), 2431–2442 (2016).
4. Y. Chen, A. Norrman, S. A. Ponomarenko, *et al.*, "Optical coherence and electromagnetic surface waves," Prog. Opt. **65**, 105–172 (2020).
5. A. A. Michelson, "The relative motion of the earth and the luminiferous ether," Am. J. Sci. **s3-22**(128), 120–129 (1881).
6. J. Tervo, T. Setälä, and A. T. Friberg, "Degree of coherence for electromagnetic fields," Opt. Express **11**(10), 1137–1143 (2003).

7. T. Setälä, J. Tervo, and A. T. Friberg, "Theorems on complete electromagnetic coherence in the space–time domain," Opt. Commun. **238**(4-6), 229–236 (2004).
8. J. Turunen, A. Halder, M. Koivurova, *et al.*, "Measurement of spatial coherence of light [Invited]," J. Opt. Soc. Am. A **39**(12), C214–C239 (2022).
9. L.-P. Leppänen, A. T. Friberg, and T. Setälä, "Temporal electromagnetic degree of coherence and Stokes-parameter modulations in Michelson's interferometer," Appl. Phys. B **122**(2), 32 (2016).
10. L.-P. Leppänen, K. Saastamoinen, A. T. Friberg, *et al.*, "Measurement of the degree of temporal coherence of unpolarized light beams," Photonics Res. **5**(3), 156–161 (2017).
11. B. Kanseri, S. Rath, and H. C. Kandpal, "Direct determination of the generalized Stokes parameters from the usual Stokes parameters," Opt. Lett. **34**(6), 719–721 (2009).
12. B. Kanseri and H. C. Kandpal, "Experimental determination of two-point Stokes parameters for a partially coherent broadband light beam," Opt. Commun. **283**(23), 4558–4562 (2010).
13. H. Partanen, B. J. Hoenders, A. T. Friberg, *et al.*, "Young's interference experiment with electromagnetic narrowband light," J. Opt. Soc. Am. A **35**(8), 1379–1384 (2018).
14. K. Saastamoinen, H. Partanen, A. T. Friberg, *et al.*, "Probing the electromagnetic degree of coherence of light beams with nannoscatterers," ACS Photonics **7**(4), 1030–1035 (2020).
15. B. Kanseri and R. Joshi, "Determination of temporal correlation properties of electromagnetic optical fields," Opt. Commun. **457**, 124710 (2020).
16. M. K. Singh and S. Datta, "Dual measurements of temporal and spatial coherence of light in a single experimental setup using a modified Michelson interferometer," Rev. Sci. Instrum. **92**(10), 105109 (2021).
17. F. J. Torcal-Milla, J. Lobera, A. M. Lopez, *et al.*, "Mach-Zehnder-based measurement of light emitting diodes temporal coherence," Optik **267**, 169722 (2022).
18. E. Wolf, "Optics in terms of observable quantities," Nuovo Cimento **12**(6), 884–888 (1954).
19. O. Korotkova and E. Wolf, "Generalized Stokes parameters of random electromagnetic beams," Opt. Lett. **30**(2), 198–200 (2005).
20. J. Tervo, T. Setälä, A. Roueff, *et al.*, "Two-point Stokes parameters: interpretation and properties," Opt. Lett. **34**(20), 3074–3076 (2009).
21. J. W. Goodman, *Introduction to Fourier Optics*, 3rd ed. (McGraw-Hill, 1996).
22. D. Goldstein, *Polarized Light*, 2nd ed. (CRC, 2003).
23. J. J. Gil and R. Ossikovski, *Polarized Light and the Mueller Matrix Approach*, 2nd ed. (CRC, 2022).